

Monomer Reactivities and Kinetics in Radical Copolymerization of Hydroxystyrene Derivatives and *tert*-Butyl (Meth)acrylate

Hiroshi Ito,* Charlie Dalby,¹ Andrew Pomerantz,² Mark Sherwood, Rikiya Sato,³ R. Sooriyakumaran, Kip Guy,⁴ and Greg Breyta

IBM Almaden Research Center, 650 Harry Road, San Jose, California 95120

Received November 16, 1999; Revised Manuscript Received April 25, 2000

ABSTRACT: Monomer reactivity ratios in radical copolymerization of 4-hydroxystyrene derivatives with *tert*-butyl acrylate and methacrylate have been determined by nonlinear regression as well as by the Kelen–Tüdös graphic method. The hydroxystyrene derivatives employed in the study included 4- and 3-hydroxystyrenes, 4- and 3-acetoxystyrenes, and 4-*tert*-butoxycarbonyloxystyrene. The electron-rich 4-hydroxystyrene is unique as its copolymerization with the electron-deficient acrylate monomers is more alternating. The simulation of the copolymerization on the basis of the reactivity ratios has been shown to fully describe the copolymerization behavior and copolymer structures. The kinetics of radical copolymerization of 4-acetoxystyrene with *tert*-butyl (meth)acrylate has been studied in detail using a gas chromatographic procedure and also by in situ ¹H NMR spectroscopy. The kinetics behavior has shown an excellent agreement with the computer simulation of the copolymerization using the reactivity ratio values determined on the basis of the terminal model.

Introduction

Microelectronics technologies have shown a remarkable progress in the past 20 years, which has been made possible by advancement of resist materials used in microlithographic imaging. Chemical amplification resists designed on the basis of photochemically induced acid-catalyzed reactions have recently replaced the novolac/diazonaphthoquinone resist in mass production of logic and memory devices by deep UV (248 nm, KrF excimer laser) lithography.^{5–7} Phenolic polymers based on poly(4-hydroxystyrene) (P4HOST) partially protected with acid-labile groups are currently the material of choice for the 248 nm lithographic technology.⁸

Commercialization of resists for mass device production requires a continuous and reproducible supply of component materials such as the above-mentioned phenolic polymers. Our deep UV positive resist named ESCAP which is a foundation of some of the today's commercial resists employs a copolymer of 4-hydroxystyrene (4HOST) with *tert*-butyl acrylate (TBA).^{9,10} The copolymer synthesis involves radical copolymerization of TBA with 4HOST or with protected 4HOST such as 4-acetoxystyrene (4ACOST), 4-*tert*-butoxycarbonyloxystyrene (BOCST),¹¹ or 4-*tert*-butyl(dimethyl)silyloxystyrene¹² followed by selective deprotection. Thermal deprotection of poly(BOCST-*co*-TBA) in the solid state or in solution was not selective enough to afford clean poly(4HOST-*co*-TBA). Although we were able to cleanly remove the silyl protecting group using fluorides without cleaving the *tert*-butyl ester functionality, the lack of the availability of the silyl-protected monomer precluded its use in our ESCAP polymer preparation. To ensure a robust resin synthesis, we have decided to study in detail the radical copolymerization behavior of these systems. *tert*-Butyl methacrylate (TBMA) as well as 3-acetoxystyrene (3ACOST) and 3-hydroxystyrene (3HOST) were also included in this investigation. Monomer reactivity ratios, simulation of the copolymerizations as a function of the conversion and feed ratio on the basis of the reactivity ratios, and kinetics of the copolymerizations as studied by gas chromatography

(GC) and in situ ¹H NMR spectroscopy are reported in this paper.

Experimental Section

Materials. 4ACOST was obtained from Hoechst Celanese (currently TriQuest) and BOCST from Eastman Kodak. 4HOST was prepared by base hydrolysis of 4ACOST.¹³ 3ACOST was synthesized by the Wittig reaction using 3-hydroxybenzaldehyde as a starting compound and purified by column chromatography (silica, *n*-hexane/CH₂Cl₂ = 5/1). 3HOST was obtained by base hydrolysis of 3ACOST and purified by distillation. TBMA and TBA were obtained from commercial sources and purified according to the known procedure. 2,2'-Azobis(isobutyronitrile) (AIBN) was purified by recrystallization from methanol and benzoyl peroxide (BPO) by reprecipitation from chloroform into methanol. Tetrahydrofuran (THF) used in the Wittig reaction was refluxed over Na and distilled. Toluene, ethylbenzene, 2-propanol (IPA), and propylene glycol methyl ether acetate (PMA) were used without further purification.

Copolymerization. Radical copolymerization of the protected HOST monomers with acrylates was carried out in toluene using 1–2.5 mol % of AIBN or BPO as the initiator at 50 or 60 °C for 1–2 h. IPA and PMA were used as the polymerization solvent for the HOST copolymerizations. All the copolymerizations were terminated at low conversions, typically <10%, to allow the use of the differential copolymerization equation for the reactivity ratio determination. Representative copolymerization procedures are as follows.

A mixture of 4ACOST (16.377 g, 0.1010 mol), TBMA (8.787 g, 0.0678 mol), and BPO (1.0 g, 0.0041 mol) in 25 mL of toluene was deaerated by bubbling nitrogen and heated in an oil bath at 60 °C in a nitrogen atmosphere for 50 min. After removing the flask from the oil bath, the mixture was diluted with 25 mL of acetone and precipitated in 750 mL of 85% aqueous methanol. The resulting precipitate was filtered, washed with the precipitation solvent (3 × 200 mL), and dried at 40 °C under vacuum for 18 h to give 1.1 g (4% conversion) of a powdery copolymer. The polymer was reprecipitated twice as a 10% solution in acetone in the same manner as above.

A mixture of 3HOST (1.215 g, 10.10 mmol), TBMA (1.432 g, 10.10 mmol), and AIBN (31 mg, 0.189 mmol) in 1.0 mL of IPA was heated under nitrogen at 50 °C for 1.5 h after repeating a freeze–thaw cycle three times. The copolymer was recovered by precipitation in hexanes. After reprecipitation

and drying, the polymer amounted to 330 mg (12.5% conversion).

Reactivity Ratio Determination. The copolymer compositions were determined by ^1H and inverse-gated¹⁴ ^1H -decoupled ^{13}C NMR spectroscopies. In the case of the BOCST copolymers, thermogravimetric analysis (TGA) was also conveniently employed in the compositional analysis based on the quantitative loss of isobutene and carbon dioxide at $\sim 200^\circ\text{C}$.¹¹ The low conversion (conversion exceeded 10% and reached 12.5% only in one case) allowed us to employ the differential copolymerization equation in the reactivity ratio determination. The reactivity ratio values were first calculated by using the Kelen-Tüdös method¹⁵ and then by employing the CONTOUR program developed by van Herk¹⁶ on the basis of nonlinear regression.¹⁷

Computer Simulation of Copolymerization. The copolymerization was simulated as a function of the conversion and feed ratio in terms of feed compositions, copolymer compositions, sequence distributions, sequence lengths, etc., employing a FORTRAN program developed by Lin and Schuerch¹⁸ and later modified in-house.

Copolymerization Kinetics Analysis by GC. The kinetics of the copolymerization was studied by GC for the 4ACOST-TBA and 4ACOST-TBMA systems using AIBN as the initiator at 60°C . Ethylbenzene was selected as the polymerization solvent and as the internal standard for the GC analysis. Calibration curves were generated first by injecting known and varying amounts of monomer pairs together with ethylbenzene diluted with methanol. In addition to monitoring the monomer consumption by GC, copolymers were isolated at intervals and analyzed for yields and for their compositions by ^1H NMR. A representative example of the procedure is as follows.

In a three-necked round-bottomed flask equipped with a condenser were placed 4ACOST (34.02 g, 210 mmol), TBA (17.92 g, 140 mmol), AIBN (1.3786 g, 8.41 mmol), and ethylbenzene (50 mL). Nitrogen was bubbled into the solution to remove oxygen before the flask was lowered into an oil bath at 60°C . Samples (4.0 g) of the reaction mixture were removed at intervals of ~ 45 min as the reaction proceeded in a nitrogen atmosphere for 24 h. Each sample was immediately precipitated into methanol (100 mL) before an aliquot of supernatant was removed for monomer concentration analysis by GC. GC samples were further diluted with methanol (10:1). Each partially solidified polymer was dissolved in acetone and reprecipitated into a methanol/water (5/1) solution. The resulting solids were filtered, washed with 200 mL of the precipitation solvent, and dried overnight to produce white powdery polymers, which were subjected to compositional analysis by ^1H NMR.

Copolymerization Kinetics Analysis by ^1H NMR. In parallel to the GC procedure, we employed ^1H NMR to monitor in situ the monomer consumption and polymer buildup in an NMR tube for the 4ACOST-TBA and 4ACOST-TBMA systems. We selected dioxane-*d*₈ as the polymerization and NMR solvent for its appropriate boiling point and lack of interfering NMR resonances in the areas of interest. Removal of oxygen was needed for radical polymerization to proceed in a NMR tube. The elimination of the paramagnetic oxygen in turn resulted in longer relaxation times, which were further lengthened by the higher temperature required for polymerization. Thus, for quantitative analysis, we performed an inversion recovery experiment¹⁹ to measure the ^1H longitudinal relaxation times (T_1) of the monomers. The ^1H T_1 's were determined for each of the individual monomer resonance lines by fitting the areas to a three-parameter model of the exponential recovery curve using a commercial software package (NUTS, ACORN NMR, Inc., CA). The longest T_1 measured was ~ 35 s. Instead of waiting a full $5T_1$ between pulses, which would be required when using a $\pi/2$ pulse, a smaller tip angle of 1.4° was used for the kinetics runs, which allowed for 104 transients to be collected in 5.2 min without saturating any of the resonances. An representative example of the NMR procedure is as follows.

In a 5 mm diameter NMR tube were placed AIBN (0.0027 g, 0.016 mmol), TBMA (0.0710 g, 0.4993 mmol), 4ACOST (0.0562 g, 0.3465 mmol), and dioxane-*d*₈ (0.5778 g). The tube

Table 1. Radical Copolymerization of 3HOST with TBMA^a

3HOST mol % in feed	yield (%)	3HOST mol % in copolymer	M_w	M_n	T_g ($^\circ\text{C}$)
10	9.2	17	431 000	204 000	136
20	8.4	28	311 000	134 000	140
30	4.0	37	342 000	181 000	149
40	6.6	45	318 000	193 000	153
50	12.5	50	308 500	149 000	156
60	7.7	56	284 000	143 000	157
70	8.4	62	263 500	142 000	163
80	9.0	72	181 000	95 000	163
90	8.1	83	145 000	75 000	163

^a [Monomer] = 20 mmol, AIBN 1 mol %, IPA 1.0 mL, 50°C , 1.5 h.

was connected to a high-vacuum line, and a freeze-thaw cycle was repeated three times to completely remove oxygen. The tube was sealed off at the constriction under high vacuum and placed, after thawing, in a ^1H NMR probe maintained at room temperature. A spectrum was recorded at room temperature first to quantify the initial concentrations of the monomers and AIBN. Then, the sample tube was removed, and the probe was heated to 64°C . The sample was reintroduced after the probe temperature reequilibrated, and a free induction decay (fid) was recorded every 30 min for 16–55 h. NMR spectra thus obtained were then processed for quantitative analysis by integration. Integration of the whole resonances remained constant throughout the kinetics runs, which provided us with confidence in our parameter setting and quantitative analysis. The peak intensities were normalized to the integration value of the entire resonance range (8–0 ppm).

Measurements. ^1H NMR spectra for the kinetics studies were recorded on a Bruker AC300 spectrometer (300 MHz) at 64°C in dioxane-*d*₈. A Bruker AF250 spectrometer was also used in determination of copolymer compositions in the ^1H (250 MHz) and ^{13}C (62.9 MHz) modes. ^{13}C NMR was also run on a Bruker AM500 spectrometer for microstructure analysis at 125.8 MHz. An inverse-gated ^1H -decoupling technique was employed for quantitative analysis by ^{13}C NMR. GC analysis was performed on a Hewlett-Packard 5890 gas chromatograph equipped with a methylsilicone column (5 m \times 0.53 mm). Thermal analyses were performed on a Perkin-Elmer TGS-2 at a heating rate of $5^\circ\text{C}/\text{min}$ for TGA and on a Du Pont 910 at $10^\circ\text{C}/\text{min}$ for differential scanning calorimetry (DSC) in nitrogen. Molecular weight determination was made by gel permeation chromatography (GPC) using a Waters model 150 chromatograph equipped with 6 μm Styragel columns at 30°C in THF. The molecular weight values reported in this paper are relative to polystyrene.

Results and Discussion

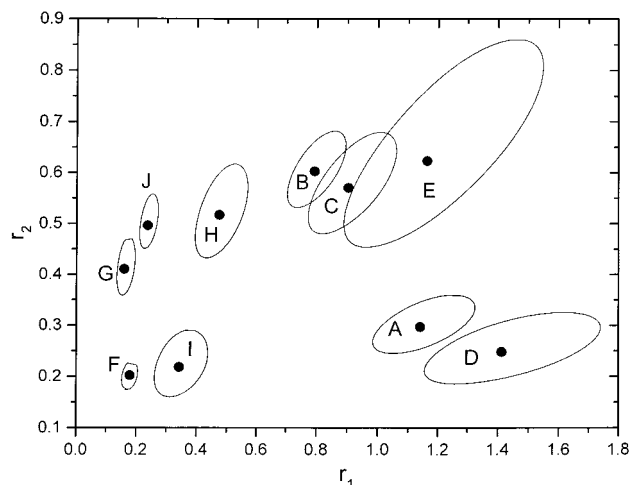
Monomer Reactivity Ratios. As an example, the results of the copolymerization of 3HOST and TBMA with 1.0 mol % of AIBN in IPA at 50°C are tabulated in Table 1. Termination after 1.5 h kept the conversion at $\sim 10\%$. Weight-average molecular weights (M_w) and glass transition temperatures (T_g) seem to be affected significantly by the copolymer compositions; an increase in the 3HOST concentration seems to result in decreased M_w and increased T_g , which may be due to the radical scavenging effect and hydrogen bonding of the phenolic functionality, respectively. The apparent molecular weight change might simply reflect a change of the hydrodynamic volume as a function of composition because the reported values are only relative to polystyrene.

Copolymerizations are in general treated, using four propagation rate constants, k_{11} , k_{12} , k_{22} , and k_{21} , on the basis of the terminal model.²⁰ However, a penultimate model has been shown in some cases²¹ to be a better

Table 2. Monomer Reactivity Ratios for HOST Derivatives (M_1) and TB(M)A (M_2) Determined by Nonlinear Regression^a

	4ACOST	3ACOST	BOCST	4HOST	3HOST
TBA	A $r_1 = 1.140$ (1.119) $r_2 = 0.297$ (0.294)		D $r_1 = 1.412$ (1.208) $r_2 = 0.248$ (0.206)	F $r_1 = 0.179$ (0.179) ^b $r_2 = 0.202$ (0.189)	
TBMA	B $r_1 = 0.792$ (0.766) $r_2 = 0.603$ (0.594)	C $r_1 = 0.903$ (0.912) $r_2 = 0.571$ (0.559)	E $r_1 = 1.162$ (1.068) $r_2 = 0.623$ (0.545)	G $r_1 = 0.159$ (0.152) ^c $r_2 = 0.410$ (0.394)	H $r_1 = 0.474$ (0.482) $r_2 = 0.517$ (0.526)

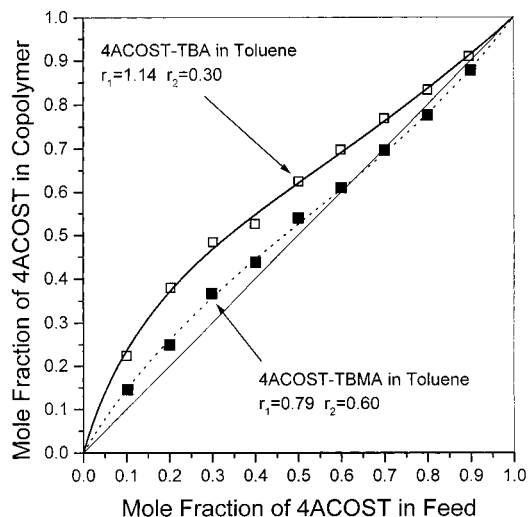
^a The values in parentheses are calculated by the Kelen–Tüdös method. ^b In IPA; $r_1 = 0.342$ (0.333) and $r_2 = 0.218$ (0.209) in PMA (I).
^c In IPA; $r_1 = 0.236$ (0.234) and $r_2 = 0.496$ (0.494) in PMA (J).

**Figure 1.** Monomer reactivity ratios and 95% joint confidence intervals for copolymerization of HOST derivatives (M_1) and (meth)acrylates (M_2); see Table 2 for identification of monomer pairs.

representation than the terminal model. It is therefore ideal if one proves that one's copolymerization can be treated with the terminal model and then proceeds to determine monomer reactivity ratios ($r_1 = k_{11}/k_{12}$ and $r_2 = k_{22}/k_{21}$). However, this is not a common practice. In this paper we determine the reactivity ratio values on the basis of the terminal model, simulate the copolymerization as a function of conversion of the monomers to polymer using the reactivity ratio values, and compare the simulation with experimental kinetics data. If the agreement between the simulation based on the terminal model and the experimental kinetics data is good, a reasonable conclusion can be made that the terminal model is an adequate expression of the copolymerization.

Monomer reactivity ratios are determined typically by the Kelen–Tüdös linear graphic method,¹⁵ as exemplified by tabulation in the *Polymer Handbook*.²² However, it has been recently recommended that reactivity ratios should be determined by using nonlinear regression and that errors in the reactivity ratio values must be expressed in 95% joint confidence intervals.^{23–25} Therefore, we have determined the monomer reactivity ratios by employing the CONTOUR program developed by van Herk¹⁶ employing the nonlinear regression procedure and also by the Kelen–Tüdös method.

For the copolymerization of the HOST derivatives (M_1) and (meth)acrylates (M_2), the monomer reactivity ratios (r_1 and r_2) and 95% joint confidence intervals determined by the nonlinear regression method are presented in Figure 1. The reactivity ratio values determined by the nonlinear regression and the Kelen–Tüdös method are tabulated and compared in Table 2. The overall agreement between the values determined by the two procedures has been found to be excellent in

**Figure 2.** Mole fractions of 4ACOST in copolymer and in feed for 4ACOST–TBA (□) and for 4ACOST–TBMA (■) in toluene and composition curves calculated for $r_1 = 1.14$ and $r_2 = 0.30$ (solid line) and $r_1 = 0.79$ and $r_2 = 0.60$ (broken line).

this study. Even in the worst case (D and E), the Kelen–Tüdös values are within the 95% joint confidence contour.

The copolymerizations involving the meta isomers were carried out at 50 °C while the others were at 60 °C. In the case of the protected HOST (4ACOST and BOCST) with TBA, the r_1 values are larger than unity and the r_2 values significantly smaller, indicating that the styrenic monomer reacts faster than the acrylate toward both the styrene and acrylate radicals. Replacement of TBA with TBMA in the copolymerization with the protected HOST results in introduction of a more azeotropic character as illustrated by the copolymer composition curves in Figure 2 for 4ACOST. This azeotropic tendency seems to prevail in all the TBMA copolymerizations with the protected HOST derivatives examined; $r_1 \approx r_2 \approx 1$.

Comparison of protected and free HOST monomers is also interesting as demonstrated in Figure 3 for the TBA systems. In the HOST copolymerizations, both r_1 and r_2 values are significantly smaller than unity in the copolymerization with either TBA or TBMA, indicating that the cross-propagation is several times faster than the self-propagation and thus providing a significantly alternating character to the HOST copolymerizations. The alternating tendency seems slightly stronger in IPA than in PMA, judging from the smaller r_1 and r_2 values in the former. The copolymerization of 3HOST with TBMA has a more azeotropic character.

Alfrey–Price Q and e values¹⁸ for 4ACOST and TBMA can be found in the literature; $Q = 1.35$ and $e = -0.8$ for 4ACOST,¹⁹ and $Q = 0.76$ and $e = 0.24$ for TBMA.²⁰ The monomer reactivity ratios can be calculated using these Q – e values as $r_1 = 0.773$ and $r_2 = 0.439$. The

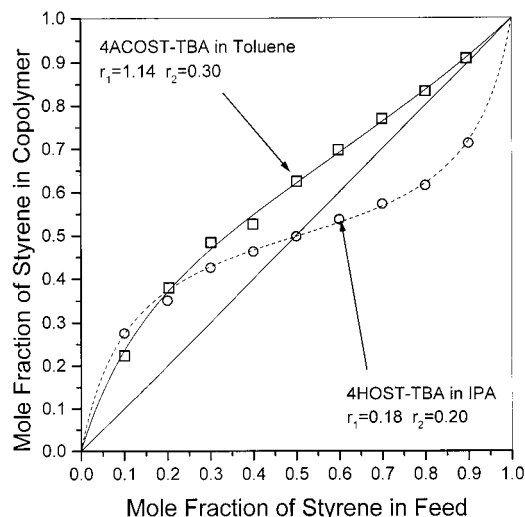


Figure 3. Mole fractions of styrenic monomer in copolymer and in feed for 4ACOST-TBA in toluene (\square) and 4HOST-TBA in IPA (\circ) and composition curves calculated for $r_1 = 1.14$ and $r_2 = 0.30$ (solid line) and for $r_1 = 0.18$ and $r_2 = 0.20$ (broken line).

calculated and experimentally determined r_1 values agree well, but our r_2 value is somewhat smaller than the calculation. From the literature $Q-e$ values of TBMA and our reactivity ratios, the resonance and electronic parameters for 4ACOST can be calculated as $Q = 1.03$ and $e = -0.62$. The $Q-e$ values for BOCST, 3ACOST, and 3HOST calculated in the same fashion are as follows: $Q = 1.06$ and $e = -0.33$ for BOCST, $Q = 1.10$ and $e = -0.57$ for 3ACOST, and $Q = 1.10$ and $e = -0.95$ for 3HOST. 4HOST has been copolymerized with a number of vinyl monomers.²⁹ Kato et al. determined reactivity ratios and calculated Q and e values for the copolymerization of 4HOST with styrene and methyl methacrylate (MMA); $Q = 1.52$ and $e = -1.03$ with styrene, and $Q = 1.14$ and $e = -1.16$ with MMA.³⁰ The $Q-e$ values of 3HOST reported by Kato are $Q = 1.10$ and $e = -0.80$ (with styrene as a comonomer) and $Q = 1.02$ and $e = -0.93$ (with MMA as a comonomer),³⁰ which agree well with the calculated values shown above. The reactivity ratios reported by Kato for 4HOST-MMA ($r_1 = 0.25$ and $r_2 = 0.34$) are similar to our values for 4HOST-TBMA. Using the literature $Q-e$ values for 4HOST and TBMA, their reactivity ratios can be calculated as $r_1 = 0.30$ and $r_2 = 0.48$, which agree reasonably well with our values experimentally determined in PMA.

The resonance and electronic states and therefore reactivities of the protected HOST derivatives and of 3HOST are more or less similar to those of styrene. In contrast, the highly electron-rich 4HOST bearing a strongly electron-donating para-OH group has a propensity toward alternating copolymerization with electron-deficient acrylates.

Simulation of Copolymerization. Once experimentally determined, the reactivity ratios can be used to simulate the entire copolymerization as a function of the feed ratio as well as of the conversion in terms of the monomer consumption, copolymer composition, sequence distribution, sequence length, etc. Thus, the copolymerization simulation based on the reactivity ratio values can be indispensable as it can provide fundamental but often ignored information regarding depletion of one monomer during the course of poly-

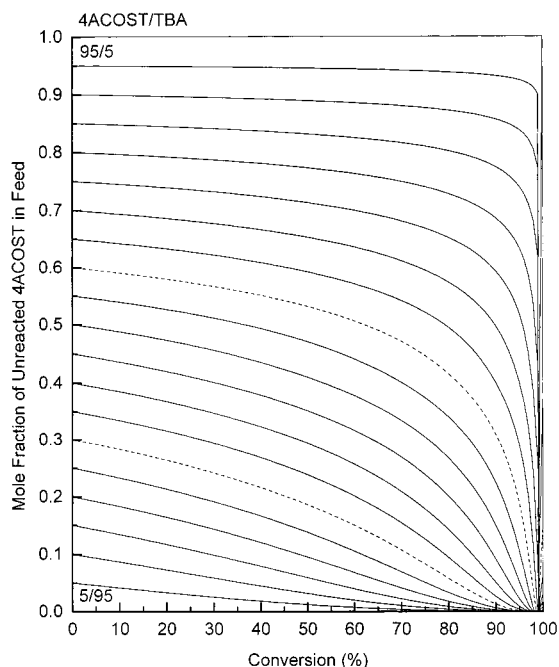


Figure 4. Mole fraction of unreacted 4ACOST in feed simulated as a function of conversion at initial feed ratio increment of 5% for 4ACOST-TBA in toluene ($r_1 = 1.14$ and $r_2 = 0.30$).

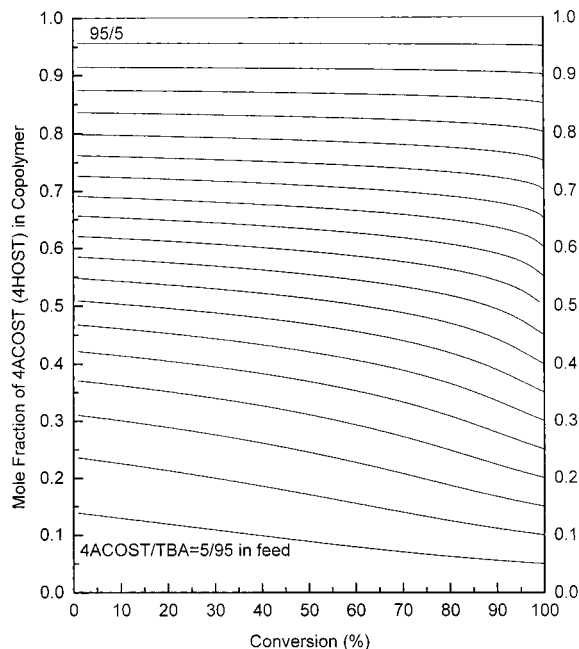


Figure 5. Mole fraction of 4ACOST (4HOST after base hydrolysis) in copolymer simulated as a function of conversion at initial feed ratio increment of 5% for 4ACOST-TBA in toluene ($r_1 = 1.14$ and $r_2 = 0.30$).

merization and homogeneity of copolymers produced (random vs blocky), for example.

In Figures 4 and 5 are presented the mole fractions of 4ACOST remaining in the feed and incorporated in the copolymer, respectively, as a function of conversion from 0 to 100% at the feed ratio increment of 5% for the copolymerization of 4ACOST with TBA in toluene at 60 °C. Figure 4 indicates that a target composition of 4ACOST/TBA = 65/35 could be obtained from a rather narrow feed ratio range of 55/45 to 65/35. The 55/45 feed ratio could produce the target composition only at a low

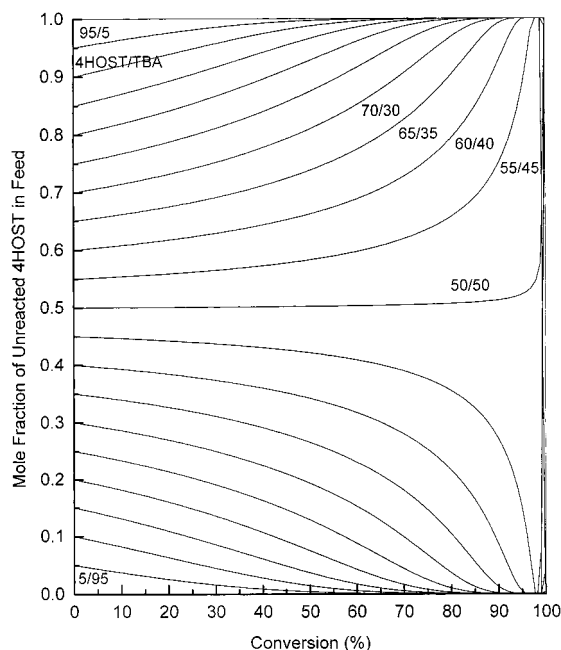


Figure 6. Mole fraction of unreacted 4HOST in feed simulated as a function of conversion at initial feed ratio increment of 5% for 4HOST–TBA in IPA ($r_1 = 0.18$ and $r_2 = 0.20$).

conversion of <20% and the 65/35 composition at the maximum conversion of 100%. Higher conversions are desirable economically. However, pushing a copolymerization to high conversions could result in exhaustive consumption of one monomer and introduction of blockiness in the copolymer. Figure 5 indicates that faster-reacting 4ACOST might be completely consumed at about 98% conversion. Therefore, it appears logical to lower the ACOST concentration in the feed from 65% toward 60% and to terminate the copolymerization at 80–90% conversion, which would ensure the formation of homogeneously random copolymers free of excessively long sequences of one monomer.

Figures 6 and 7 present the simulated dependence of the feed and copolymer compositions, respectively, on the conversion for varying initial feed ratios for the 4HOST–TBA system in IPA at 60 °C. In this monomer combination, the target copolymer composition of 4HOST/TBA = 65/35 could be prepared from the feed ratio ranging from 85/15 (0% conversion) to 65/35 (100% conversion). In this case the TBA concentration in feed must be lower than in the 4ACOST system for the target composition. The monomer consumption curve presented in Figure 6 indicates that the minor component TBA would be completely depleted only above 90% conversion in the case of the 65/35 feed ratio. However, a long sequence of the HOST unit begins to grow at relatively low conversions in this case, as demonstrated by the plots of the sequence length of 4HOST instantaneously incorporated in the copolymer against the conversion. To avoid any heterogeneity in the copolymer composition, it would be advisable to increase the 4HOST concentration in the feed toward 70% and terminate the copolymerization at <85%.

Thus, although the HOST–TBA copolymers with the same final composition (and molecular weight) could be obtained from the copolymerization of TBA with HOST or with 4ACOST followed by hydrolysis, the microstructures (sequence distributions) of the two copolymers could be very different. For example, poly(4HOST-*co*-TBA)s containing 31% TBA could be prepared by

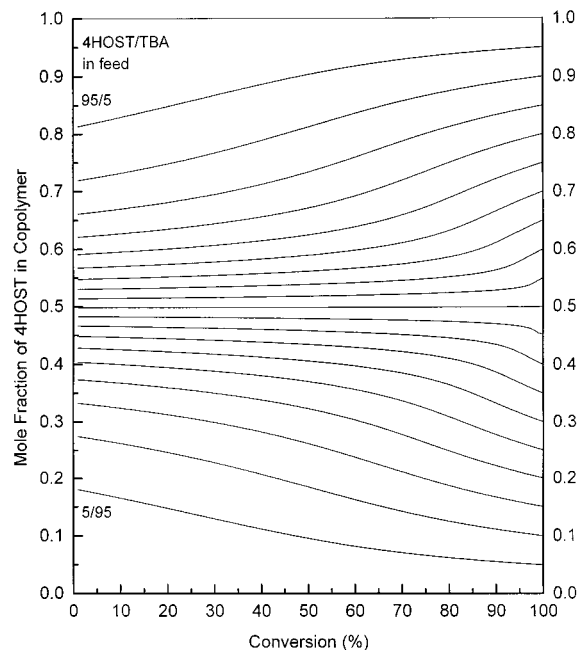


Figure 7. Mole fraction of 4HOST in copolymer simulated as a function of conversion at initial feed ratio increment of 5% for 4HOST–TBA in IPA ($r_1 = 0.18$ and $r_2 = 0.20$).

terminating the copolymerizations at about 80% conversion from feed ratios of 4ACOST/TBA = 65/35 and 4HOST/TBA = 75/25. The concentrations of the acrylate-centered triads and styrene-centered pentad sequences were calculated and are compared for these two copolymers with the same compositions. In the copolymer made directly from 4HOST, the alternating SAS triad (A for acrylate and S for styrene) is the dominant sequence. The number-average sequence length of TBA = 1 amounts to 95% of the total TBA concentration in the copolymer, with the sequence length of 2 and 3 sharply falling to ~5 and ~0%, respectively. The copolymer made from 4ACOST contains a significant concentration of the AAS triad sequence. The number-average sequence length of TBA = 1 still amounts to ~80%, but the sequence length distribution is broader than in the copolymer made from 4HOST, with the number-average sequence length gradually falling (~15% for 2, ~3% for 3, ~1% for 4, and ~0% for 5). ^{13}C NMR can nicely detect this difference in the sequence distributions as shown in Figure 8. The aromatic C1 resonances of the two polymers with the same compositions are significantly different, most likely reflecting the differences in pentad sequences. While the ester carbonyl resonance is dominated by a peak at the lowest field in the case of the 4HOST system, the polymer made from 4ACOST exhibits a large shoulder and a third peak at a slightly higher field in the carbonyl ^{13}C resonance, which again agree well with our simulation results. The quaternary carbon resonance of the copolymer made from 4ACOST exhibits a splitting pattern similar to the carbonyl resonance, although reversed in the chemical shift, while the copolymer made from 4HOST essentially gives a single resonance.

Copolymerization Kinetics As Studied by GC. The kinetics of the copolymerization of 4ACOST with TBA and TBMA initiated with AIBN at 60 °C was investigated by GC, using ethylbenzene as the polymerization solvent and as the internal standard for the GC analysis. Calibration curves were generated to correlate the GC peak area ratios of the monomers to

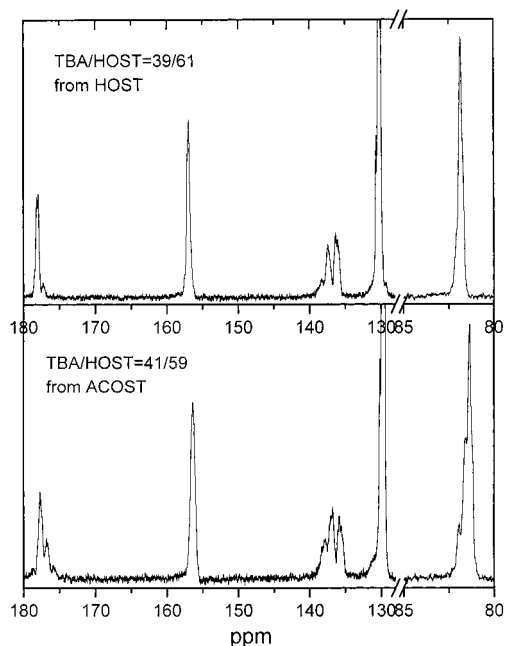


Figure 8. The 125 MHz ^{13}C NMR spectra of poly(4HOST-*co*-TBA)s of similar compositions made from 4HOST (top) and from 4ACOST (bottom) in methanol- d_4 .

ethylbenzene to the actual concentrations (mol/L), giving excellent linear fitting. The calibration was necessary as the sensitivity of the response of each monomer to our GC detector was significantly different.

Figure 9 presents the time-conversion curves for the 4ACOST/TBA feed ratio of 28.6/71.4 ($[\text{4ACOST}]_0 = 2.0$ mol/L and $[\text{TBA}]_0 = 5.0$ mol/L). The concentrations of the two monomers (mol/L) are plotted as a function of the polymerization time (T in minutes), which can be nicely fitted with exponential decay curves:

$$\log [\text{TBA}] = 0.703 - 9.75 \times 10^{-4} T$$

$$\log [\text{4ACOST}] = 0.286 - 1.91 \times 10^{-3} T$$

In a similar fashion, the kinetics of the monomer consumption for the 4ACOST/TBA feed ratio of 60/40 ($[\text{4ACOST}]_0 = 4.2$ mol/L and $[\text{TBA}]_0 = 2.8$ mol/L) can be expressed as follows:

$$\log [\text{TBA}] = 0.421 - 6.26 \times 10^{-4} T$$

$$\log [\text{4ACOST}] = 0.537 - 8.51 \times 10^{-4} T$$

Thus, it is clear that 4ACOST is consumed faster than TBA. Because of the faster consumption of 4ACOST, the feed becomes more and more enriched with TBA as the polymerization proceeds and the TBA concentration becomes greater than the 4ACOST concentration in the mixture after about 400 min of polymerization even when the TBA was a smaller component in the initial feed. In the case of the feed containing a smaller amount of more reactive 4ACOST (4ACOST/TBA = 3/7), the 4ACOST concentration remains lower and becomes lower and lower as a function of the polymerization time, and finally 4ACOST has been almost completely consumed after about 1500 min.

The copolymer yields are plotted as a function of the polymerization time for the 4ACOST/TBA feed ratio of 6/4 in Figure 10. The yields were calculated from the monomer consumption determined by GC and also by

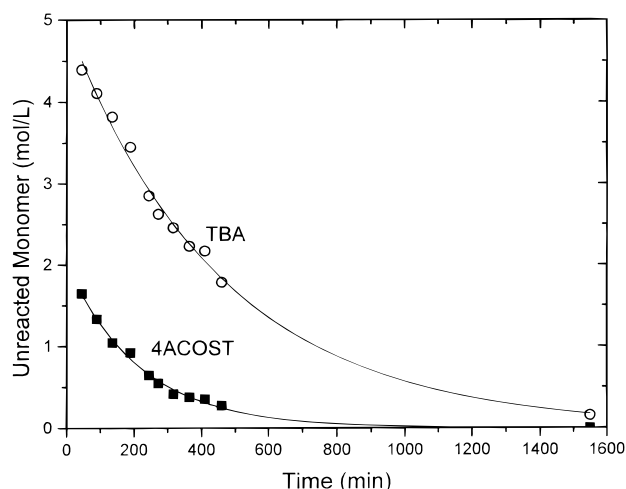


Figure 9. Monomer consumption kinetics curves generated by GC analysis for copolymerization of 4ACOST and TBA in ethylbenzene at 60 °C. $[\text{4ACOST}]_0 = 2.0$ mol/L and $[\text{TBA}]_0 = 5.0$ mol/L; AIBN = 2.4 mol %.

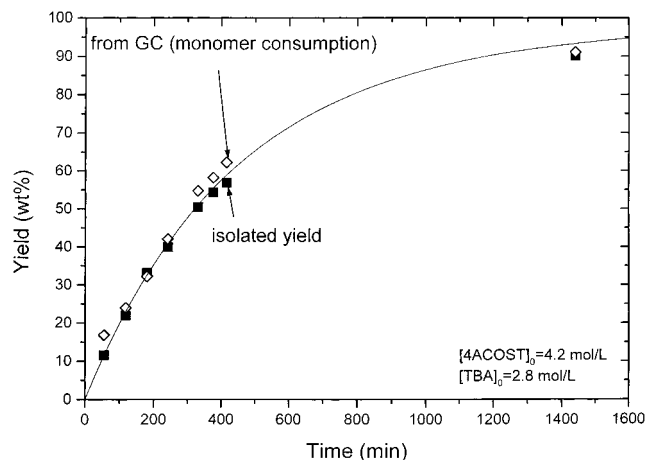


Figure 10. Time dependence of copolymer yields determined by polymer isolation and calculated from monomer consumption analysis by GC for copolymerization of 4ACOST and TBA in ethylbenzene at 60 °C. $[\text{4ACOST}]_0 = 4.2$ mol/L and $[\text{TBA}]_0 = 2.8$ mol/L; AIBN = 2.4 mol %.

isolating copolymers by precipitation at intervals. The isolated yields are slightly lower than the yields calculated on the basis of the monomer consumption perhaps due to some material loss during the isolation/recovery process, but their agreement is excellent. The time-conversion curve can be nicely expressed by an exponential decay as is the case with the 4ACOST/TBA feed ratio of 30/70.

In the case of the 4ACOST/TBMA = 57.9/42.1 feed ratio ($[\text{4ACOST}]_0 = 3.82$ mol/L, $[\text{TBMA}]_0 = 2.78$ mol/L), the monomer consumption kinetics can be expressed by the following equations:

$$\log [\text{TBMA}] = 0.397 - 4.84 \times 10^{-4} T$$

$$\log [\text{4ACOST}] = 0.471 - 5.38 \times 10^{-4} T$$

Thus, the rates of polymerization for the two monomers are very similar in this case, and the feed and copolymer compositions remain essentially constant throughout the course of copolymerization as demonstrated in Figure 11. The compositions of the copolymers were determined by subjecting the copolymer samples isolated at intervals to 250 MHz ^1H NMR analysis.

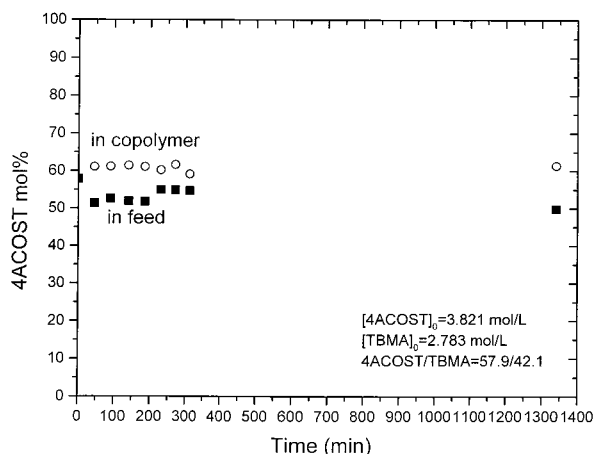


Figure 11. Time dependence of 4ACOST concentration in feed (GC analysis) and in copolymer (^1H NMR analysis) for copolymerization of 4ACOST and TBMA in ethylbenzene at 60°C . $[\text{4ACOST}]_0 = 3.82 \text{ mol/L}$ and $[\text{TBMA}]_0 = 2.78 \text{ mol/L}$; AIBN = $2.4 \text{ mol } \%$.

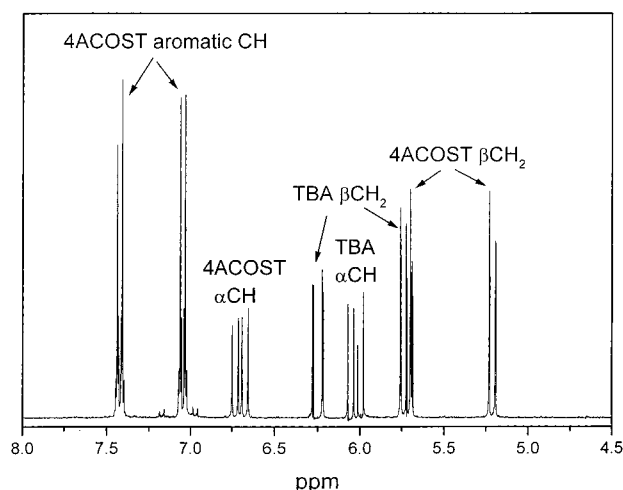


Figure 12. The 300 MHz ^1H NMR spectrum of a kinetics sample consisting of 4ACOST (0.99 mol/L), TBA (0.64 mol/L), and AIBN ($2.5 \text{ mol } \%$) in dioxane- d_8 at room temperature.

Copolymerization Kinetics As Studied by in Situ ^1H NMR. As the ^1H NMR spectrum in Figure 12 indicates, the resonances for all the vinylic protons of 4ACOST and TBA (or TBMA) are well separated and could be conveniently used to monitor the consumption of these monomers. Dioxane- d_8 is a good solvent for the NMR study as its residual protons resonate only in the open area of the spectrum without interfering with any NMR signals of interest. However, one difficulty associated with this NMR experiment was long ^1H T_1 in the absence of paramagnetic oxygen. Oxygen must be removed to carry out radical polymerization in an NMR tube, which results in much longer T_1 values. Furthermore, T_1 becomes even larger at the elevated temperatures needed for polymerization. To determine the correct parameter setting for *quantitative* NMR analysis, relaxation times have been determined at 64°C (polymerization temperature) for the 4ACOST, TBA, and TBMA monomers in dioxane- d_8 and are tabulated in Table 3. The longest T_1 observed was 35 s. Waiting $5T_1$ between $\pi/2$ pulses is typically needed to avoid saturation of the resonances and to achieve good quantification, which would be impractical in our investigation. Thus, the exceedingly long T_1 prompted us to employ a smaller tip angle. After a small number of

Table 3. Relaxation Time^a of 4ACOST, TBA, and TBMA at 64°C in Dioxane- d_8

	aromatic CH	αCH	βCH_2	αCH_3	OCOCH_3	OC_4H_9
4ACOST	6.8, 13.6	10.1	3.8, 5.2		5.4	
TBA		34.0	13.2, 10.6			5.6
TBMA			6.7, 6.2	7.3		4.7

^a In seconds.

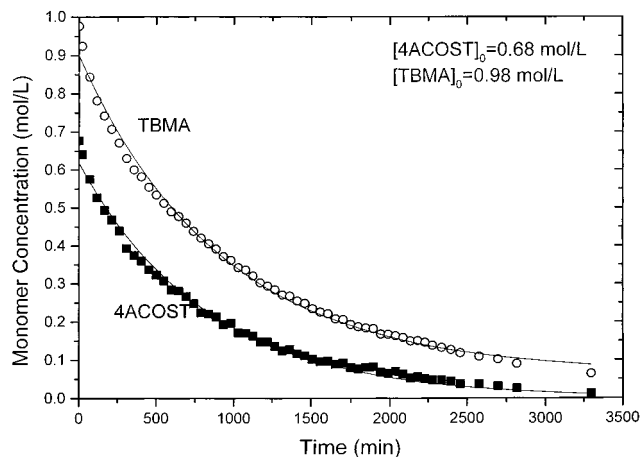


Figure 13. Monomer consumption kinetics curves generated by in situ ^1H NMR analysis for copolymerization of 4ACOST with TBMA in dioxane- d_8 at 64°C . $[\text{4ACOST}]_0 = 0.68 \text{ mol/L}$ and $[\text{TBMA}]_0 = 0.98 \text{ mol/L}$; AIBN = $1.9 \text{ mol } \%$.

pulses, the magnitude of the projection of the steady state magnetization on the z -axis immediately before the pulse is given by $M_z = M_0\{1 - \exp(-T/T_1)\}/\{[1 - \exp(-T/T_1)] \cos \beta\}$, where M_0 is the projection along the z -axis after full relaxation, T is the time before pulses, and β is the tip angle.¹⁷ Using a T of 3 s (acquisition time = 2.7 s, recycle delay = 0.3 s) and insisting that $M_z/M_0 = 0.99$, this equation predicted that the tip angle should be 2.7° . To be conservative, a tip angle of 1.4° was used during the runs, which allowed for 104 transients to be collected in 5.2 min without saturating any of the resonances.

The integration value of the whole spectral range must remain constant throughout the polymerization if the NMR parameters have been set correctly and in fact was constant. The area intensities of the resonances of interest (primarily vinyl protons) were thus normalized to the integration of the whole range. As shown in Figure 12, a spectrum was obtained first at room temperature. Because a broad aromatic resonance due to polymer grows between 6.5 and 7.3 ppm as the polymerization proceeds, the $\alpha\text{-CH}$ resonance and the high field half of the C_6H_4 AA'BB' system of 4ACOST were not included in our analysis of the monomer consumption. The low field half of the AA'BB' resonance of the aromatic protons looked well separated from the broad polymer peak but was found to be still sitting on the foot of the polymer peak, and therefore only the $\beta\text{-CH}_2$ resonances of 4ACOST were employed in the monomer consumption analysis.

The monomer consumption kinetics curves are presented in Figure 13 for the feed composition $[\text{4ACOST}]_0 = 0.677 \text{ mol/L}$ and $[\text{TBMA}]_0 = 0.976 \text{ mol/L}$, which can be rather nicely expressed by an exponential decay in the time span up to more than 2 days and to a high conversion of at least 95%. The copolymer yield (wt %) calculated from the monomer consumption is plotted as

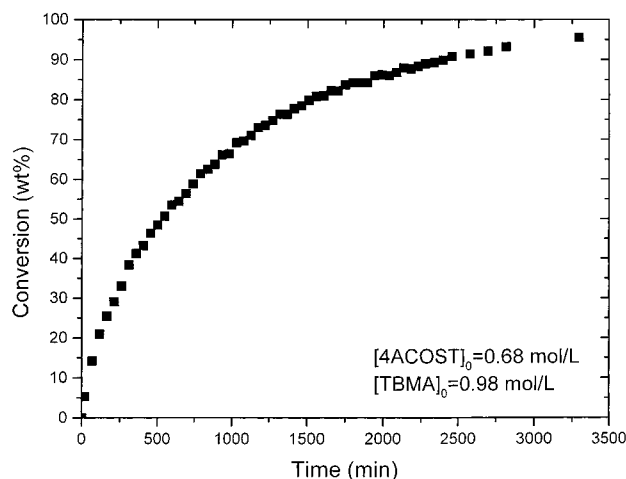


Figure 14. Time dependence of copolymer yield calculated from NMR analysis of monomer consumption for copolymerization of 4ACOST and TBMA in dioxane- d_8 at 64 °C. $[4ACOST]_0 = 0.68$ mol/L and $[TBMA]_0 = 0.98$ mol/L; AIBN = 1.9 mol %.

a function of time in Figure 14 for this 4ACOST–TBMA copolymerization. The 4ACOST concentration in the copolymer calculated from the monomer consumption remains almost constant at 45–42 mol % throughout the course of polymerization for the feed ratio of 4ACOST/TBMA = 41/59.

In Figure 15 is plotted the 4ACOST mol % in feed and in copolymer determined from the monomer consumption as a function of conversion (wt %) calculated also from the monomer consumption for the initial feed composition of $[4ACOST]_0 = 0.867$ mol/L and $[TBMA]_0 = 0.505$ mol/L (ratio 63.2/36.8). The feed and copolymer composition remained unchanged within the experimental time range (up to about 70% conversion in this case), which is consistent with all the previous discussion.

For the copolymerization of 4ACOST/TBA = 60.8/39.2 ($[4ACOST]_0 = 0.994$ mol/L and $[TBA]_0 = 0.640$ mol/L), the concentrations of the unreacted monomers are plotted against the polymerization time in a semilogarithmic scale in Figure 16. The monomer consumption kinetics can be expressed as follows:

$$\log [TBA] = -0.196 - 4.45 \times 10^{-4} T$$

$$\log [4ACOST] = -0.057 - 8.26 \times 10^{-4} T$$

4ACOST is consumed about twice more rapidly than TBA. The mole fraction of TBA in the feed almost linearly increases from 0.4 to 0.62 as the copolymerization proceeds to 72 wt % conversion after 960 min. The TBA concentration in the feed becomes greater than the 4ACOST concentration after about 350 min of polymerization.

In the case of the initial feed ratio of 4ACOST/TBA = 29.6/70.4 ($[4ACOST]_0 = 0.456$ mol/L and $[TBA]_0 = 1.082$ mol/L), the ACOST monomer becomes exhausted after about 20 h. The copolymer yield curve for this system fits well with an exponential decay and agrees well with the data obtained by GC, although the copolymerization is a little slower in the NMR experiments than in the GC investigations (~90% vs ~100% after about 27 h) because a lower monomer concentration is needed to obtain good ^1H NMR spectra.

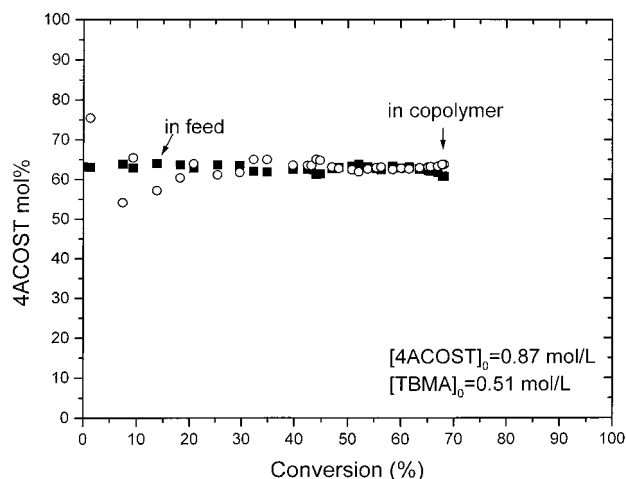


Figure 15. Time dependence of 4ACOST concentration in feed (■) and in copolymer (○) determined by in situ NMR analysis of monomer consumption for copolymerization of 4ACOST and TBMA in dioxane- d_8 at 64 °C. $[4ACOST]_0 = 0.87$ mol/L and $[TBMA]_0 = 0.51$ mol/L; AIBN = 2.3 mol %.

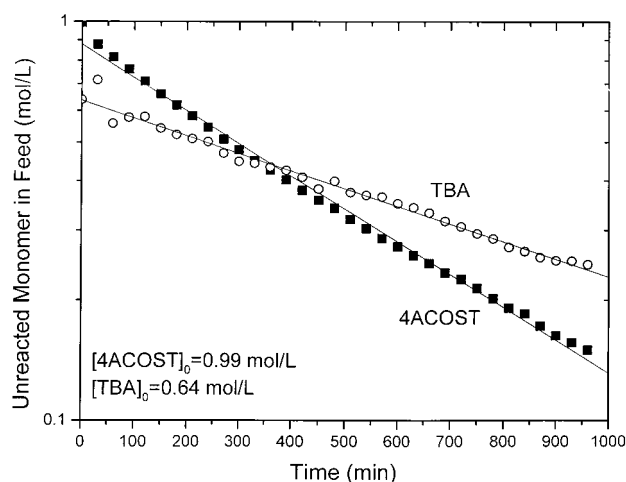


Figure 16. Semilogarithmic monomer consumption kinetics curves generated by in situ NMR analysis of copolymerization of 4ACOST with TBA in dioxane- d_8 at 64 °C. $[4ACOST]_0 = 0.99$ mol/L and $[TBA]_0 = 0.64$ mol/L; AIBN = 2.3 mol %.

The copolymer compositions can be also directly estimated from the ^1H NMR spectra of the reaction mixtures without isolating polymers by subtracting the contributions from the unreacted monomers, AIBN, and its decomposition products from the integration data of the aromatic and aliphatic regions. The 4ACOST concentration in the copolymer thus calculated is shown as a function of the polymerization time for the 4ACOST/TBA = 29.6/70.4 in Figure 17. Although there are some scatters in the low conversion region, this NMR technique allows to conveniently monitor in a single experiment not only the monomer consumption but also the composition of copolymers as they are produced.

Comparison of Experimental Kinetics Data with Simulation. Comparison of Figures 11 and 15 with Figure 4 clearly suggests that the simulation based on the reactivity ratio values agrees well with the experimental data derived from the kinetics experiments. As a more convincing and direct comparison, simulation curves of the 4ACOST concentrations in feed and copolymer are presented along with the experimental data points for the 4ACOST/TBA = 29/71 (GC) and for the 4ACOST/TBMA = 41/59 (NMR) in Figures 18 and

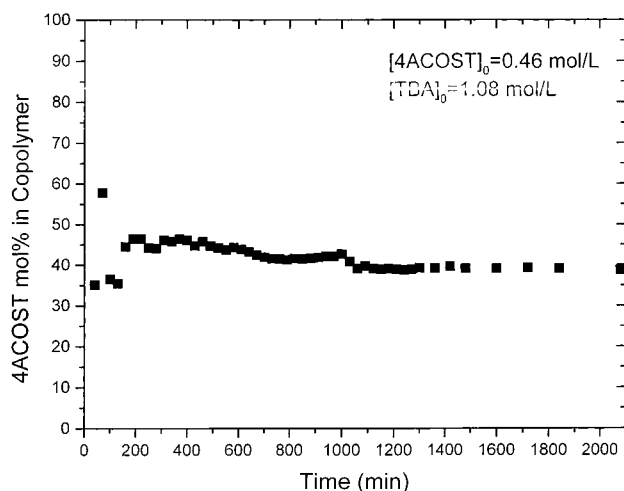


Figure 17. Time dependence of 4ACOST concentration in copolymer directly determined by in situ analyzing copolymerization of 4ACOST and TBA in dioxane- d_8 at 64 °C. $[4ACOST]_0 = 0.56$ mol/L and $[TBA]_0 = 1.08$ mol/L; AIBN = 2.3 mol %.

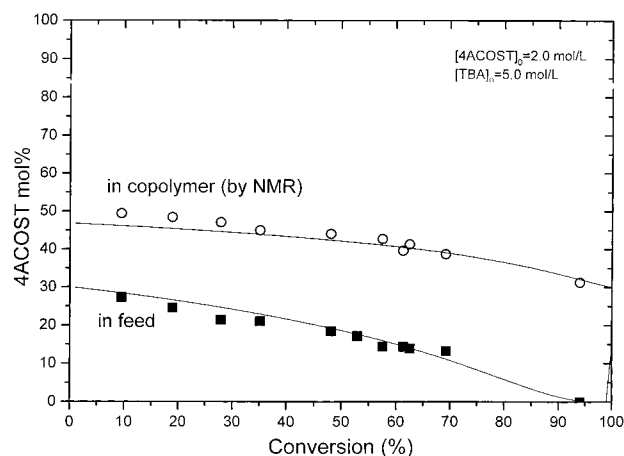


Figure 18. Conversion dependence of 4ACOST concentration in feed (determined by GC) and in copolymer (determined by 1H NMR analysis of isolated copolymers) and simulation (solid lines) based on $r_1 = 1.14$ and $r_2 = 0.30$ for copolymerization of 4ACOST and TBA. $[4ACOST]_0 = 2.0$ mol/L and $[TBA]_0 = 5.0$ mol/L.

19, respectively. In the case of the GC study (Figure 18), the copolymer compositions were determined by 1H NMR for isolated copolymers as mentioned earlier. The copolymer compositions in the kinetics studies by NMR were derived from the monomer consumption (Figure 19). The simulation was carried out at 5 mol % feed increments, and the curves shown in Figures 18 and 19 are for 4ACOST/TBA = 30/70 and 4ACOST/TBMA = 40/60. The agreements are excellent, confirming that the terminal model is an adequate expression of the copolymerization described in this paper and reinforcing the importance and usefulness of the reactivity ratio determination and simulation in understanding the copolymerization behavior, copolymer structures, sequence distributions, etc. In addition, the excellent agreement between the classical kinetics studies by GC and the NMR procedures proves the quantitative nature of the NMR analysis. The NMR method could be advantageous in many cases as it generates many data points automatically and provides compositional information on both feed and copolymer produced in a single experiment.

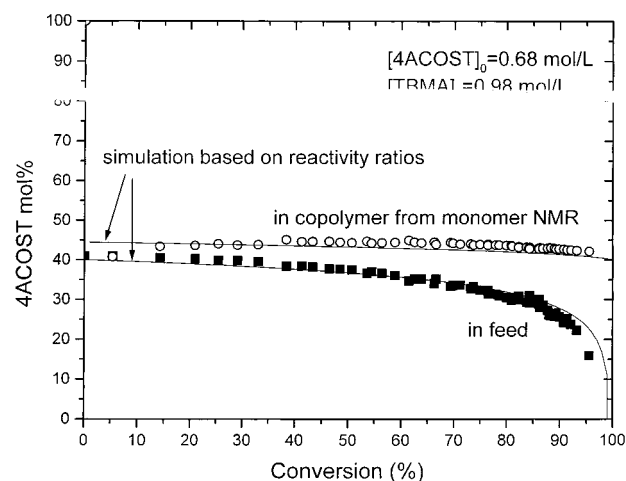


Figure 19. Conversion dependence of 4ACOST concentration in feed and in copolymer determined by 1H NMR analysis of monomer consumption and simulation (solid lines) based on $r_1 = 0.79$ and $r_2 = 0.60$ for copolymerization of 4ACOST with TBMA. $[4ACOST]_0 = 0.68$ mol/L and $[TBMA]_0 = 0.98$ mol/L.

Summary and Conclusions

Monomer reactivity ratios have been determined by nonlinear regression based on the terminal model for the copolymerizations of hydroxystyrene derivatives (4ACOST, 3ACOST, BOCST, 4HOST, and 3HOST) with *tert*-butyl acrylate and methacrylate that produce lithographically important materials. The reactivity ratios for these systems have been compared with the values for the related monomers reported in the literature. The highly electron-rich 4HOST copolymerizes with the electron-deficient acrylate monomers in a significantly alternating fashion.

These copolymerization reactions have been simulated on the basis of the experimentally determined reactivity ratios using a FORTRAN program as a function of conversion in terms of the feed composition, copolymer composition, sequence distribution, sequence length, etc. The copolymerization behavior has been described in detail on the basis of simulation. The difference in the microstructure has been demonstrated for poly(4HOST-*co*-TBA) made from 4HOST and from 4ACOST to the same compositions by the simulation and also by ^{13}C NMR analysis of the copolymers.

The kinetics of the radical copolymerization of 4ACOST with TBA and TBMA has been studied to high conversions, using GC and also by 1H NMR, varying the feed ratio. The two procedures showed excellent agreements. In the case of the GC procedure, copolymers were isolated at intervals and analyzed for yield and composition. The monomer consumption, feed composition, copolymer composition, and yield have been described as a function of polymerization time in detail.

The compositional changes of the feed and copolymer have been replotted against copolymer yield for direct comparison with the simulation based on the reactivity ratios, demonstrating an excellent agreement between the experimental data and the simulation. This study clearly indicates that the reactivity ratios can be employed to accurately describe the copolymerization behavior and copolymer structures by simulation and that copolymerization of the HOST derivatives with (meth)acrylates can be adequately described by the terminal model. The influence of the penultimate units may be insignificant in the copolymerization between electron-deficient acrylates and electron-rich styrenes.

The kinetics studies by GC or NMR can also provide valuable information regarding the copolymerization reaction as well as copolymer composition as a function of time for a fixed feed ratio. The ^1H NMR procedure is very simple and highly useful as it can generate a large number of data points automatically and can analyze not only the feed composition but also the copolymer composition (may be difficult in some cases) in one experiment without requiring calibration.

Acknowledgment. This research was supported in part by the NSF Materials Science and Engineering Research Center for Polymer Interfaces and Macromolecular Assemblies (Grant 9808677) to Stanford University and by NSF GOALI Grant CHE-9625628 (Surface and Analytical Chemistry of Materials) to San Jose State University. The CONTOUR program was generously provided by Dr. van Herk, which is gratefully acknowledged.

References and Notes

- (1) CPIMA Summer Intern, 1998.
- (2) NSF/SJSU Summer Intern, 1998.
- (3) Visiting Scientist from Yamagata University, Japan, 1995–1996.
- (4) Summer Intern, 1991.
- (5) Reichmanis, E.; Houlihan, F. M.; Nalamasu, O.; Neenan, T. X. *Chem. Mater.* **1991**, *3*, 394.
- (6) MacDonald, S. A.; Willson, C. G.; Fréchet, J. M. J. *Acc. Chem. Res.* **1994**, *27*, 151.
- (7) Ito, H. In *Desk Reference of Functional Polymers*; Arshady, R., Ed.; American Chemical Society: Washington, DC, 1997; p 341.
- (8) Ito, H. *Solid State Technol.* **1996**, *36* (7), 164.
- (9) Ito, H.; Breyta, G.; Hofer, D.; Sooriyakumaran, R.; Petrillo, K.; Seeger, D. *J. Photopolym. Sci. Technol.* **1994**, *7*, 433.
- (10) Ito, H.; Sherwood, M. *Proc. SPIE* **1999**, *3678*, 104.
- (11) Fréchet, J. M. J.; Eichler, E.; Ito, H.; Willson, C. G. *Polymer* **1983**, *24*, 995.
- (12) Packirisamy, S.; Hirao, A.; Nakahama, S. *J. Polym. Sci., Part A: Polym. Chem.* **1989**, *27*, 2811.
- (13) Hirao, A.; Yamaguchi, K.; Takenaka, K.; Suzuki, K.; Nakahama, S. *Makromol. Chem., Rapid Commun.* **1982**, *3*, 941.
- (14) Freeman, R.; Hill, H. D. W.; Kaptein, R. *J. Magn. Reson.* **1972**, *7*, 327.
- (15) Kelen, T.; Tüdös, F. *J. Macromol. Sci., Chem.* **1975**, *A9*, 1.
- (16) CONTOUR. van Herk, A. M., available from the author: Laboratory of Polymer Chemistry, Eindhoven University of Technology, PO Box 513, 5600 MB Eindhoven, The Netherlands, 1996. *J. Chem. Educ.* **1995**, *72*, 138.
- (17) Bevington, P. R. *Data Reduction and Error Analysis for the Physical Sciences*; McGraw-Hill: New York, 1969.
- (18) Lin, J. W.-P.; Schuerch, C. *Macromolecules* **1973**, *6*, 320.
- (19) Ernst, R. R.; Bodenhausen, G.; Wokaer, A. *Principles of Nuclear Magnetic Resonance in One and Two Dimensions*; Clarendon Press: Oxford, 1987.
- (20) Mayo, F. R.; Lewis, F. M. *J. Am. Chem. Soc.* **1944**, *66*, 1594.
- (21) Coote, M. L.; Davis, T. P. *Macromolecules* **1999**, *32*, 3626.
- (22) Greenley, R. Z. *Polymer Handbook*, 3rd ed.; Wiley: New York, 1989; p 153.
- (23) Tidwell, P. W.; Mortimer, G. A. *J. Polym. Sci., Part A* **1965**, *3*, 369.
- (24) O'Driscoll, K. F.; Reilly, P. M. *Makromol. Chem., Macromol. Symp.* **1987**, *10/11*, 355.
- (25) van Herk, A. M. *J. Chem. Educ.* **1995**, *72*, 138.
- (26) Alfrey, T.; Price, C. C. *J. Polym. Sci.* **1947**, *2*, 101.
- (27) Danusso, F.; Ferruti, P.; Marabelli, C. G. *Chim. Ind. (Milan)* **1965**, *47* (6), 585.
- (28) *Polymer Handbook*; Brandrup, J., Immergut, E. H., Eds.; J. Wiley & Sons: New York, 1975.
- (29) *Vinylphenol*; Research Center of Maruzen Petrochemical Co., Ltd., Ed.; Kyoiku Shuppan Center: Tokyo, 1991.
- (30) Kato, M. *J. Polym. Sci., Part A-1* **1969**, *7*, 2175.

MA9919357